Oxidation of Ammonia in Osmium Polypyridyl Complexes

George M. Coia,[†] Konstantinos D. Demadis,[‡] and Thomas J. Meyer*[,§]

Department of Chemistry, Venable and Kenan Laboratories, CB 3290,
University of North Carolina at Chapel Hill, Chapel Hill, North Carolina 27599-3290

Received January 18, 2000

The oxidations of *cis*- and *trans*-$[Os^{III}(tpy)(Cl)_2(NH_3)](PF_6)$, *cis*-$[Os^{II}(bpy)_2(Cl)(NH_3)](PF_6)$, and $[Os^{II}(tpy)(bpy)(NH_3)](PF_6)_2$ have been studied by cyclic voltammetry and by controlled-potential electrolysis. In acetonitrile or in acidic, aqueous solution, oxidation is metal-based and reversible, but as the pH is increased, oxidation and proton loss from coordinated ammonia occurs. *cis*- and *trans*-$[Os^{III}(tpy)(Cl)_2(NH_3)](PF_6)$ are oxidized by four electrons to give the corresponding Os^{VI} nitrido complexes, $[Os^{VI}(tpy)(Cl)_2(N)]^+$. Oxidation of $[Os(tpy)(bpy)(NH_3)](PF_6)_2$ occurs by six electrons to give $[Os(tpy)(bpy)(NO)](PF_6)_3$. Oxidation of *cis*-$[Os^{II}(bpy)_2(Cl)(NH_3)](PF_6)$ at pH 9.0 gives *cis*-$[Os^{II}(bpy)_2(Cl)(NO)](PF_6)_2$ and the mixed-valence form of the μ-N_2 dimer {*cis*-$[Os(bpy)_2(Cl)]_2(\mu\text{-}N_2)$}$(PF_6)_3$. With NH_4^+ added to the electrolyte, *cis*-$[Os^{II}(bpy)_2(Cl)(N_2)](PF_6)$ is a coproduct. The results of pH-dependent cyclic voltammetry measurements suggest Os^{IV} as a common intermediate in the oxidation of coordinated ammonia. For *cis*- and *trans*-$[Os^{III}(tpy)(Cl)_2(NH_3)]^+$, Os^{IV} is a discernible intermediate. It undergoes further pH-dependent oxidation to $[Os^{VI}(tpy)(Cl)_2(N)]^+$. For $[Os^{II}(tpy)(bpy)(NH_3)]^{2+}$, oxidation to Os^{IV} is followed by hydration at the nitrogen atom and further oxidation to nitrosyl. For *cis*-$[Os^{II}(bpy)_2(Cl)(NH_3)]^+$, oxidation to Os^{IV} is followed by N−N coupling and further oxidation to {*cis*-$[Os(bpy)_2(Cl)]_2(\mu\text{-}N_2)$}$^{3+}$. At pH 9, N−N coupling is competitive with capture of Os^{IV} by OH^- and further oxidation, yielding *cis*-$[Os^{II}(bpy)_2(Cl)(NO)]^{2+}$.

Introduction

Oxidation of polypyridyl Ru^{II} and Os^{II} aqua complexes proceeds via sequential electron/proton loss to give high-oxidation-state oxo complexes, as shown in eq 1 (bpy is 2,2′-bipyridine, and py is pyridine).[1]

$$cis\text{-}[Ru^{II}(bpy)_2(py)(H_2O)]^{2+} \underset{+H^+,\,+e^-}{\overset{-H^+,\,-e^-}{\rightleftharpoons}} cis\text{-}[Ru^{III}(bpy)_2(py)(OH)]^{2+} \underset{+H^+,\,+e^-}{\overset{-H^+,\,-e^-}{\rightleftharpoons}} cis\text{-}[Ru^{IV}(bpy)_2(py)(O)]^{2+} \quad (1)$$

The Ru^{IV}, Ru^{V}, and Ru^{VI} oxo products that result are potent and efficient oxidants, capable of oxidizing olefins to epoxides and alcohols to aldehydes.[2,3] Despite their reactivity, salts of the oxo complexes can be isolated as solids and studied in solution for extended periods. The high oxidation states are stabilized by σ and π donation from the oxo ligand.

A related reactivity exists for other ligands that bind through an electronegative atom from which protons are easily lost, especially nitrogen ligands. For example, oxidative dehydrogenation of ammonia is a general route to the formation of metal−ligand multiple bonds,[4] examples including

$$[Os^{III}(NH_3)_6]^{3+} \xrightarrow[+H_2O]{-3e^-,\,-3H^+,\,-NH_3} trans\text{-}[Os^{VI}(NH_3)_4(H_2O)(N)]^{3+} \quad (2)$$

$$trans\text{-}Cr^{III}(porph)(OH)(NH_3) \xrightarrow{-2e^-,\,-2H^+,\,-2H_2O} Cr^{V}(porph)(N) \quad (3)$$

where porph = 5,10,15,20-tetra-*p*-tolylphophyrinato dianion

$$Os^{II}(tpy)(Cl)_2(NH_3) \underset{+4e^-,\,+3H^+}{\overset{-4e^-,\,-3H^+}{\rightleftharpoons}} [Os^{VI}(tpy)(Cl)_2(N)]^+ \quad (4)$$

$$W(Tp')(CO)_2(NH_2) \xrightarrow{-1H^+,\,-2e^-} [W(Tp')(CO)_2(NH)]^+ \quad (5)$$

where Tp′ = hydrido-tris(3,5-dimethyl-1-pyrazolyl)borate

$$W(Cp^*)(CH_3)_3(NH_2) \xrightarrow{-H^+,\,-e^-} W(Cp^*)(CH_3)_3(NH) \quad (6)$$

where Cp* = pentamethyl cyclopentadienyl

The examples in eqs 2−6 (see refs 5−9, respectively) are relatively rare because the amido (NH^{2-}), imido (NH^{2-}), and nitrido (N^{3-}) products that form are reactive. A typical following reaction is hydration and further oxidation to give nitrosyl products. For example, $[M^{II}(tpy)(bpy)(NH_3)]^{2+}$ (M = Ru and

[†] Present address: Division of Chemistry and Chemical Engineering, California Institute of Technology, Pasadena, CA 91125. E-mail: gcoia@its.caltech.edu.

[‡] Present address: Nalco Chemical Company, Global Water Research, One Nalco Center, Naperville, IL 60563-1198. E-mail: kdemadis@nalco.com.

[§] Present address: Los Alamos National Laboratories, MS A127, Los Alamos, NM 87545. E-mail: tjmeyer@lanl.gov.

(1) (a) Moyer, B. A.; Meyer, T. J. *J. Am. Chem. Soc.* **1978**, *100*, 3601. (b) Moyer, B. A.; Meyer, T. J. *Inorg. Chem.* **1981**, *20*, 436. (c) Binstead, R. A.; Moyer, B. A.; Samuels, G. J.; Meyer, T. J. *J. Am. Chem. Soc.* **1981**, *103*, 2899. (d) Takeuchi, K. J.; Thompson, M. S.; Pipes, D. W.; Meyer, T. J. *Inorg. Chem.* **1984**, *23*, 1845. (e) Binstead, R. A.; Meyer, T. J. *J. Am. Chem. Soc.* **1987**, *109*, 3287. (f) Dobson, J. C.; Helms, J. H.; Doppelt, P.; Sullivan, B. P.; Hatfield, W. E.; Meyer, T. J. *Inorg. Chem.* **1989**, *28*, 2200. (g) Marmion, M. E.; Leising, R. A.; Takeuchi, K. J. *J. Coord. Chem.* **1988**, *19*, 1.

(2) (a) Lai, T. S.; Zhang, R.; Cheung, K.-K.; Kwong, H. L.; Che, C.-M. *Chem. Commun.* **1998**, 1583. (b) Stultz, L. K.; Binstead, R. A.; Reynolds, M. S.; Meyer, T. J. *J. Am. Chem. Soc.* **1995**, *117*, 2520. (c) Dobson, J. C.; Seok, W. K.; Meyer, T. J. *Inorg. Chem.* **1986**, *25*, 1513.

10.1021/ic0000505 CCC: $19.00
Published on Web 04/26/2000

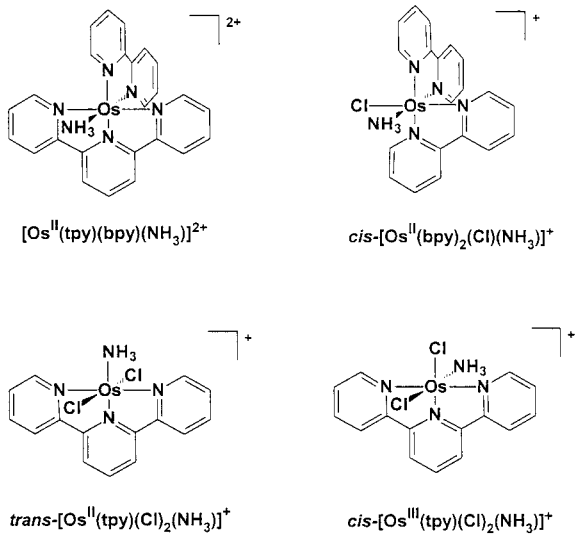

Figure 1. Structures of the ammine complexes used in the study (bpy = 2,2′-bipyridine, tpy = 2,2′,6′:2″-terpyridine).

Os, tpy = 2,2′,6′:2″-terpyridine) undergoes six-electron oxidation in water to give the corresponding nitrosyl product $[M^{II}(tpy)(bpy)(NO)]^{3+}$.[10] Although intermediates are seldom isolable, valuable information has been gained by trapping experiments. Oxidation of $[Os(tpy)(bpy)(NH_3)]^{2+}$ in the presence of secondary amines or ammonia affords hydrazido or dinitrogen complexes, respectively.[11,12]

Taube and co-workers studied oxidation of the Os^{III} haloammines $[Os(NH_3)_5(X)]^{2+}$, *cis*- and *trans*-$[Os(NH_3)_4(X)_2]^{+}$, and *mer*-$Os(NH_3)_3(X)_3$ (X = Cl, Br, and I).[5] Their observations suggest that proton loss and disproportionation at Os^{IV} and proton loss from coordinated NH_3 are controlling features in the chemistry of this process.

In this paper, we report on the oxidation of the series of Os^{II} monoammine complexes shown in Figure 1. These complexes display a remarkable diversity of reactivity toward the oxidation of coordinated ammonia. Part of this work also involves a reinvestigation of the electrochemistries of $[Os(tpy)(bpy)(NH_3)]^{2+}$ and *cis*-$[Os(tpy)(Cl)_2(NH_3)]^{+}$, which were reported previously.[7,10,17]

Experimental Section

Measurements. Proton NMR spectra were acquired using Bruker AC200 (200 MHz) and WM250 (250 MHz) spectrometers. FT-IR spectra were recorded on a Mattson Galaxy Series 5000 instrument at 2 cm^{-1} resolution. UV−visible spectra were recorded on a Hewlett-Packard model 8452A diode array spectrophotometer. Spectra in the near-IR region were recorded on a Cary model 14 spectrometer. Elemental microanalyses were performed by Oneida Research Services, Inc., or by Galbraith Laboratories, Inc.

Resonance Raman spectra were obtained using an intensified charge-coupled device (ICCD) detection system (Princeton model 576G/RB) with an ST 130 detector controller interfaced to an 80386-based computer. Data were collected and processed using Princeton Instruments CSMA software. Laser excitation of 441.6 nm was provided by a Liconix model 4240NB HeCd laser, while excitation of 488 nm was provided by a Spectra-Physics 165 Ar^{+} laser. Spectra were obtained from solutions that were millimolar in the metal complex in NMR tubes with the laser beam focused onto the sample by a glass lens. The scattered light was collected with a 135° backscattering geometry with a conventional camera lens, and dispersion was achieved with a SPEX 1877 triple spectrometer equipped with a 1200-groove/mm grating. The ICCD was calibrated against known Raman bands of solvents.

Electrochemical measurements and preparative electrolyses were conducted using a PAR model 273 potentiostat. For aqueous voltammetry, a 2.0-mm-diameter glassy carbon disk working electrode[13] and a saturated sodium chloride calomel reference electrode (SSCE) were used. For nonaqueous measurements, the working electrode was a 1.0-mm platinum disk, and the reference was a silver wire immersed in a CH_3CN solution that was 0.01 M in $AgNO_3$ and 0.1 M in tetra-*n*-butylammonium hexafluorophosphate (TBAH). In all cases, the auxiliary electrode was a coil of platinum wire. Three-compartment cells were used, with sintered glass disks separating the compartments containing reference, working, and auxiliary electrodes. For cyclic voltammetry experiments employing scan rates greater than 2 V/s, an analog waveform generator (PAR model 175) was used to supply the triangle wave to the potentiostat. The analog current and voltage outputs of the potentiostat were sampled by a Tektronix model 2230 digital storage oscilloscope (100 MHz).

The solution in the working compartment was deoxygenated with a stream of argon. Acetonitrile was distilled from calcium hydride prior to use in electrochemical experiments. TBAH was recrystallized three times from absolute ethanol and dried in vacuo. Buffers for aqueous voltammetry were prepared by neutralizing solutions of reagent A with solid or concentrated reagent B until the desired pH was reached. For pH 7.6−10.0, A = 0.3 M NaOH and B = H_3BO_3; for pH 5.8−7.8, A = 0.5 M NaH_2PO_4 and B = NaOH; for pH 3.6−5.6, A = 0.5 M CH_3COOH and B = NaOH; for pH 2.2−3.8, A = 0.075 M potassium hydrogen phthalate and B = H_2SO_4; and for pH 1−2.2, A = 0.5 M Na_2SO_4 and B = H_2SO_4. Electrolytes of pH <1 consisted of solutions of H_2SO_4.

Spectroelectrochemical titrations were conducted in a three-compartment cell that was modified by incorporation of a 1-cm quartz cuvette into the central (working) compartment. The open end of the cuvette, designed for use with a serum cap, was secured to the bottom of the glass cell by means of a short length of heat-shrink plastic tubing. The working electrode was a platinum mesh that was held at constant potential by means of a PAR model 175 potentiostat. Efficient convection was achieved by bubbling solvent-saturated argon through the working compartment during electrolysis. Argon was introduced through a Teflon cannula which was extended to the mouth of the cuvette, but which was above the optical path. Spectra were recorded at fixed time intervals using a Hewlett-Packard model 8452A diode-array spectrophotometer.

(3) (a) Roecker, L.; Meyer, T. J. *J. Am. Chem. Soc.* **1987**, *109*, 746. (b) Marmion, M. E.; Takeuchi, K. J. *J. Chem. Soc., Dalton Trans.* **1988**, 2385. (c) Muller, J. G.; Acquaye, J. H.; Takeuchi, K. J. *Inorg. Chem.* **1992**, *31*, 4552. (d) Moyer, B. A.; Thompson, M. S.; Meyer, T. J. *J. Am. Chem. Soc.* **1980**, *102*, 2310. (e) Seok, W. K.; Dobson, J. C.; Meyer, T. J. *Inorg. Chem.* **1988**, *27*, 3. (f) Thompson, M. S.; Meyer, T. J. *J. Am. Chem. Soc.* **1982**, *104*, 5070. (g) Thompson, M. S.; DeGiovanni, W. F.; Moyer, B. A.; Meyer, T. J. *J. Org. Chem.* **1984**, *49*, 4972. (h) Cheng, J. Y.; Cheung, K.-K.; Che, C.-M. *Chem. Commun.* **1997**, 1443. (i) Fung, W. H.; Yu, W. Y.; Che, C.-M. *J. Org. Chem.* **1998**, *63*, 2873.
(4) (a) Nugent, W. A.; Mayer, J. A. *Metal−Ligand Multiple Bonds*; Wiley: New York, 1988; Chapter 3. (b) Che, C.-M. *Pure Appl. Chem.* **1995**, *67*, 225.
(5) Buhr, J. D.; Winkler, J. R.; Taube, H. *Inorg. Chem.* **1980**, *19*, 2416.
(6) Buchler, J. W.; Dreher, C.; Lay, K. L.; Raap, A.; Gresonde, K. *Inorg. Chem.* **1983**, *22*, 879. Porphyrine complexes of manganese (Hill, C. L.; Hollander, F. J. *J. Am. Chem. Soc.* **1982**, *104*, 7318) and osmium [Buchler, J. W.; Kokisch, W.; Smith, P. D. *Struct. Bonding (Berlin)* **1978**, *34*, 79] undergo the same reaction.
(7) Pipes, D. W.; Bakir, M.; Vitols, S. E.; Hodgson, D. J.; Meyer, T. J. *J. Am. Chem. Soc.* **1990**, *112*, 5507.
(8) Perez, P. J.; Luan, L.; White, P. S.; Brookhart, M.; Templeton, J. L. *J. Am. Chem. Soc.* **1992**, *114*, 7928.
(9) Glassman, T. E.; Vale, M. G.; Schrock, R. R. *Organometallics* **1991**, *10*, 4046.
(10) Murphy, W. R.; Takeuchi, K. J.; Barley, M. H.; Meyer, T. J. *Inorg. Chem.* **1986**, *25*, 1041.
(11) Coia, G. M.; White, P. S.; Meyer, T. J.; Wink, D. A.; Keefer, L. K.; Davis, W. M. *J. Am. Chem. Soc.* **1994**, *116*, 3649.
(12) Coia, G. M.; Wink, D. A.; Devenney, M.; White, P. S.; Meyer, T. J. *Inorg. Chem.* **1997**, *36*, 2341.

(13) Bioanalytical Systems, West Lafayette, IN.

Preparations. The preparation of chloride and hexafluorophosphate salts of *cis*- and *trans*-$[Os(tpy)(Cl)_2(N)]^+$ is described elsewhere.[14][14] Cation exchange chromatography was conducted using Sephadex CM C-25 as the column support. Sparingly water-soluble salts were dissolved in 9:1 water−acetonitrile mixtures to assist in loading. Pure products were precipitated by addition of NH_4PF_6 or $NaPF_6$ to the eluant. Stirring was maintained for 45 min at 0 °C before collection. The solids were washed with ice-cold water followed by anhydrous diethyl ether.

$[Os(tpy)(bpy)(NH_3)](PF_6)_2$ was prepared by a modification of a published procedure.[10] $[Os(tpy)(bpy)(NO_2)](PF_6)$[15] (1.25 g) was stirred in 100 mL of 0.2 M aqueous HCl and 10 mL of acetonitrile until both solid and solution became yellow, which indicated conversion of the nitro to the nitrosyl complex. The suspension was then stirred for 5 h with several pieces of freshly amalgamated zinc. After filtration and removal of the acetonitrile by rotary evaporation, 1 g of NH_4PF_6 was added, and the mixture was stirred at 0 °C for 1 h. The dark solid was collected by filtration and purified by cation exchange chromatography, using 0.2 M NH_4Cl as the eluant. Yield: 1.34 g (92%). ^{1}H NMR (200 MHz, acetone-d_6): δ 3.79 (s, br, 3H, NH_3), 7.05 (t, 1H, $J = 6.2$), 7.35−7.50 (m, 3H), 7.68 (q, 2H, $J = 8.2$), 7.85−8.20 (m, 6H), 8.61 (t, 3H, $J = 8.9$), 8.76 (d, 2H, $J = 7.9$), 8.92 (d, 1H, $J = 7.6$), 9.67 (d, 1H, $J = 5.4$).

***cis*-$[Os(bpy)_2(Cl)(NH_3)](PF_6)$** was prepared by the method of Buckingham et al.,[16] modified as follows. The product solution was subjected to a brief period of rotary evaporation at 60 °C in order to remove traces of dissolved ammonia. Aqueous NH_4PF_6 was added to induce precipitation. Removal of ammonia was necessary because the product is air-sensitive in basic, aqueous solution. The solid was collected by filtration and purified by chromatography on neutral alumina with a 2:1 acetonitrile−toluene mixture as the eluant. After evaporation of the solvent, the black, microcrystalline product was rinsed with diethyl ether and dried in vacuo. ^{1}H NMR (200 MHz, CD_3CN): δ 6.64 (t, 2H), 7.2−7.8 (m, 8H), 8.21 (d, 2H), 8.39 (d, 2H), 8.76 (d, 1H), 9.61 (d, 1H).

***trans*-$[Os(tpy)(Cl)_2(NH_3)](PF_6)$.** *trans*-$[Os(tpy)(Cl)_2(N)](PF_6)$ (91 mg) and trifluoroacetic acid (166 μL) were dissolved in 50 mL of acetonitrile. Fine copper granules (1 g) were added, and the mixture was stirred vigorously for 30 min. The solution rapidly became red-brown, but with continued stirring, the Os^{II} ammine precipitated as a fine, black powder. The suspension containing the product was decanted from the metal. Complete recovery of the precipitate was accomplished by sonication of the copper granules in a few milliliters of water. The product was taken to dryness by rotary evaporation, which also resulted in oxidation to Os^{III}. The residue was dissolved in a 9:1 water−acetonitrile mixture and purified by cation exchange chromatography with 0.1 M NaCl as the eluant. ^{1}H NMR (200 MHz, CD_3CN): featureless because of paramagnetism. Anal. Calcd (found): C, 27.4 (27.3); N, 8.5 (8.9); H, 2.2 (2.0).

***cis*-$[Os(tpy)(Cl)_2(NH_3)](PF_6)$.** This complex was prepared by two methods. The first is exactly as described above for the trans isomer, except that *cis*-$[Os(tpy)(Cl)_2(N)](PF_6)$ was used as the starting material. The second method is a modification of a literature procedure.[7,17] *trans*-$[Os(tpy)(Cl)_2(N)]Cl$ (106 mg) was dissolved in 30 mL of 3 M HCl. Several pieces of amalgamated zinc were added, and the mixture was stirred vigorously in a stoppered flask. The pale yellow solution quickly became red-brown. With continued stirring, the Os^{II} ammine precipitated as a fine, black solid. After 30 min, the zinc was removed, and 500 mg of NH_4PF_6 was added. The suspension was stirred, open to the air, for 1 h, which resulted in oxidation to Os^{III}. The mixture was chilled to 0 °C and stirred for an additional 1 h. The solid product was collected by filtration and purified by cation exchange chromatography. The eluant was 0.1 M NaCl. ^{1}H NMR (200 MHz, CD_3CN): featureless because of paramagnetism. Anal. Calcd (found): C, 27.4 (27.3); N, 8.5 (8.6); H, 2.2 (1.6).

{*cis*-$[Os(bpy)_2(Cl)]_2(\mu\text{-}N_2)$}$(PF_6)_2$. The pH of a solution 0.13 M in H_3BO_3 and 0.50 M in NaCl was adjusted to 9.2 by addition of sodium hydroxide. In 150 mL of this solution was dissolved 168 mg of *cis*-$[Os(bpy)_2(Cl)(NH_3)](PF_6)$. The solution was oxidized electrochemically at a reticulated vitreous carbon electrode at +0.65 V. Approximately 91 C was passed before the current decayed to 2% of its initial value. The potential was switched to +0.30 V for reduction. Approximately 1.3 C was passed before the current decayed to the baseline. The anolyte was withdrawn and cooled to 0 °C, and NH_4PF_6 (0.5 g) was added. The olive-green solid that precipitated was collected by filtration and washed with ice-cold water and diethyl ether. It was purified by cation exchange chromatography using 0.2 M NaCl as the eluant. ^{1}H NMR (200 MHz, CD_3CN): complex superposition of peaks from 7.0 to 9.5 ppm because of the presence of two diastereomers (denoted A and B) in a ratio of 3:2. The more easily resolved peaks occur at δ 7.05 (t, $^4/_5$H, B), 7.15 (t, $^6/_5$H, A), 7.30 (d, 1H, A + B), 8.70 (d, $^2/_5$H, B), 9.13 (d, $^3/_5$H, A), 9.49 (d, br, 1H, A + B). Anal. Calcd (found): C, 34.5 (34.2); N, 10.0 (10.2); H, 2.3 (2.0).

***cis*-$[Os(tpy)(Cl)_2(N_2)](PF_6)$.** The pH of a 0.3 M aqueous H_3BO_3 solution was adjusted to 9.2 by addition of concentrated ammonium hydroxide. In 50 mL of this solution was dissolved 53.5 mg of *cis*-$[Os(bpy)_2(Cl)(NH_3)](PF_6)$. The remaining manipulations were carried out either in darkness or with the aid of a red light. The solution was oxidized electrochemically at a reticulated vitreous carbon electrode at +0.65 V. Approximately 39 C was passed before the current decayed to 2% of its initial value. The anolyte was withdrawn and cooled to 0 °C, and 500 mg of $NaPF_6$ was added with stirring. The red-brown solid that precipitated was collected by filtration and washed with ice-cold water and diethyl ether. It was purified by cation exchange chromatography using 0.1 M NaCl as the eluent. The product was stored in a desiccator and protected from light at all times. ^{1}H NMR (200 MHz, CD_3CN): δ 6.90 (t, 2H), 7.1−8.0 (m, 8H), 8.30 (d, 2H), 8.41 (d, 2H), 8.73 (d, 1H), 9.68 (d, 1H). Anal. Calcd (found): C, 33.8 (33.6); N, 11.8 (11.2); H, 2.3 (2.4). IR (KBr): ν_{N_2} 2099 cm^{-1}.

Results

Preparation of Osmium Ammines. Literature preparations were available for salts of $[Os(tpy)(bpy)(NH_3)]^{2+}$ and *cis*-$[Os(bpy)_2(Cl)(NH_3)]^+$. Additional chromatographic procedures were used to provide analytically pure samples. An isomer of $[Os(tpy)(Cl)_2(NH_3)]^+$ had been prepared previously by reduction of *trans*-$[Os(tpy)(Cl)_2(N)](Cl)$ in acidic, aqueous solution.[7,17] It was later found that, under these conditions, *trans*-$[Os(tpy)(Cl)_2(N)]Cl$ undergoes rapid isomerization to the cis isomer, suggesting that the isolated ammine complex was also cis.[14] Isomerization of $[Os(tpy)(Cl)_2(N)]^+$ occurs much more slowly in acetonitrile and other polar organic solvents. This allowed the corresponding trans ammine to be prepared by reduction of the trans nitrido precursor in acetonitrile. The general reaction is

$$\textit{cis}\text{- or }\textit{trans}\text{-}[Os^{VI}(tpy)(Cl)_2(N)]^+ \xrightarrow[2.\ O_2]{1.\ Cu,\ H^+} \textit{cis}\text{- or }\textit{trans}\text{-}[Os^{III}(tpy)(Cl)_2(NH_3)]^+ \quad (7)$$

Evidence for successful isolation of the two isomers was indirect. Infrared spectra are similar. Both are paramagnetic, having featureless ^{1}H NMR spectra. The complexes were isolated in the Os^{III} forms because the Os^{II} forms are air-sensitive. Attempts to grow X-ray quality crystals were unsuccessful. However, elemental analysis confirms that each salt is $[Os^{III}(tpy)(Cl)_2(NH_3)](PF_6)$, and bands containing the separate isomers were eluted from the cation exchange column completely resolved. The efficacy of the chromatographic method was verified by separation of a mixture of the purified cis and trans products under conditions identical to those used in the purification. The mixture was easily resolved, with the cis isomer eluting slightly faster than the trans.

(14) Williams, D. S.; Coia, G. M.; Meyer, T. J. *Inorg. Chem.* **1995**, *34*, 586.
(15) Pipes, D. W.; Meyer, T. J. *Inorg. Chem.* **1984**, *23*, 2466.
(16) Buckingham, D. A.; Dwyer, F. P.; Goodwin, H. A.; Sargeson, A. M. *Aust. J. Chem.* **1964**, *17*, 325.
(17) Ware, D. C.; Taube, H. *Inorg. Chem.* **1991**, *30*, 4598.

Table 1. $E_{1/2}$ Values for Os(III/II) and Os(IV/III) Couples[a]

	$E_{1/2}$ Os(III/II), V		$E_{1/2}$ Os(IV/III), V	
ammine complex	H_2O[b]	CH_3CN[c]	H_2O[b]	CH_3CN[c]
$[Os(tpy)(bpy)(NH_3)]^{2+}$	+0.41	+0.68	–	–
cis-$[Os(bpy)_2(Cl)(NH_3)]^+$	+0.04	+0.21	+1.23	+1.69[d]
trans-$[Os(tpy)(Cl)_2(NH_3)]^+$	−0.18	−0.10	+0.88	+1.18
cis-$[Os(tpy)(Cl)_2(NH_3)]^+$	−0.16	−0.11	+0.89	+1.18

[a] Values are referenced vs SSCE, which is 0.24 V vs NHE. [b] Measured in 0.2 M H_2SO_4. [c] With 0.1 M TBAH. [d] Irreversible oxidation, $E_{p,a}$ given.

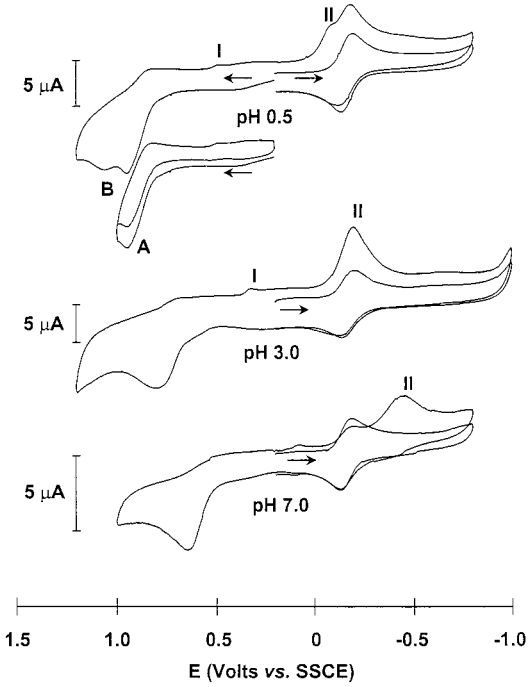

Figure 2. Cyclic voltammograms of *cis*-$[Os(tpy)(Cl)_2(NH_3)](PF_6)$, ~0.2 mM in aqueous solution. Potentials are vs SSCE. The scan rate is 100 mV/s.

Electrochemistry in Acetonitrile and Acid. Each complex exhibited one or more stages of quasireversible oxidation in acetonitrile or water at pH >0.

Os(III/II). The Os(III/II) couples were chemically reversible in acetonitrile and in strongly acidic aqueous solutions. $E_{1/2}$ values are listed in Table 1.

Os(IV/III). Os(IV/III) waves appear in cyclic voltammograms of *cis*- and *trans*-$[Os(tpy)(Cl)_2(NH_3)]^+$ and *cis*-$[Os(bpy)_2(Cl)(NH_3)]^+$ both in acetonitrile and in acid. Potentials are listed in Table 1. $[Os(tpy)(bpy)(NH_3)]^{3+}$ is not oxidized to Os^{IV} within the range of potentials accessible in acetonitrile or water.

Electrochemistry in Neutral and Basic Media. *cis*-[Os(tpy)(Cl)$_2$(NH$_3$)]PF$_6$. As shown in Figure 2, at pH 0.5, a quasireversible Os(IV/III) wave appears at $E_{1/2} = +0.89$ V (wave A). Scan reversal past this wave reveals a small, irreversible wave at $E_{p,c} = +0.65$ V (wave I). This wave is pH-dependent, with $E_{p,c}$ decreasing by 60−70 mV per unit increase in pH until pH 7.0.

The Os(III → IV) wave is followed by an irreversible Os(IV → VI) oxidation wave at approximately +1.1 V (wave B) which, because it gives the nitrido complex as the product, is a two-electron process.

$$cis\text{-}[Os^{IV}(tpy)(Cl)_2(NH_3)]^{2+} \xrightarrow{-3H^+,\,-2e^-} cis\text{-}[Os^{VI}(tpy)(Cl)_2(N)]^+ \quad (8)$$

On a return scan, the nitrido complex undergoes irreversible reduction at approximately −0.2 V (wave II) to Os^{IV}.

$$cis\text{-}[Os^{VI}(tpy)(Cl)_2(N)]^+ \xrightarrow{+3H^+,\,+2e^-} cis\text{-}[Os^{IV}(tpy)(Cl)_2(NH_3)]^+ \quad (9)$$

The Os(IV → VI) wave is pH-dependent with $E_{p,a}$ decreasing by 110−120 mV per unit increase in pH from pH 0.5 to 3.0. By pH 3.0, it overlaps with the Os(III → IV) wave, and only a single wave is observed, which, by inference, is a three-electron Os(III → VI) oxidation. Os(VI → IV) reduction is also pH-dependent with $E_{p,c}$ decreasing 50−60 mV per unit increase in pH from pH 0.5 to 7.0. At pH 3, it overlaps with the Os(III → II) reduction wave.

The Os^{IV} intermediate is unstable. Electrolysis past the Os(IV/III) wave results in complete oxidation to $Os^{VI}{\equiv}N^+$ with $n = 3$. The instability of Os^{IV} can be explained by disproportionation, as shown in eq 10,[7]

$$3\ cis\text{-}[Os^{IV}(tpy)(Cl)_2(NH_3)]^{2+} \rightarrow cis\text{-}[Os^{VI}(tpy)(Cl)_2(N)]^+ + 2\ cis\text{-}[Os^{III}(tpy)(Cl)_2(NH_3)]^+ + 3H^+ \quad (10)$$

followed by further oxidation of Os^{III} to Os^{IV}. Disproportionation of Os^{IV} once it is formed may also explain the small peak current for the Os(IV → III) reduction at wave I. In CH_3CN, irreversible one-electron reduction of *cis*-$[Os^{VI}(tpy)(Cl)_2(N)]^+$ occurs at $E_{p,c} = -0.3$ V to give *cis*-$Os^{V}(tpy)(Cl)_2(N)$.

$$cis\text{-}[Os^{VI}(tpy)(Cl)_2(N)]^+ \xrightarrow{+e^-} cis\text{-}Os^{V}(tpy)(Cl)_2(N) \quad (11)$$

Once Os^V is formed, it undergoes rapid N···N coupling.[18]

$$2cis\text{-}Os^{V}(tpy)(Cl)_2(N) \rightarrow cis,cis\text{-}(tpy)(Cl)_2Os^{II}(N_2)Os^{II}(Cl)_2(tpy) \quad (12)$$

***trans*-[Os(tpy)(Cl)$_2$(NH$_3$)](PF$_6$).** Limited solubility and adsorption complicated measurements on this salt. A pattern of waves similar to that of the cis isomer is observed (Figure 3), but there are significant differences. At pH 0.5, Os(III → IV) oxidation at $E_{p,a} = +0.88$ V (wave A) is completely irreversible. The corresponding Os(IV → III) reduction occurs at wave I, where $E_{p,c} = +0.25$ V. Oxidation of Os^{III} is pH-dependent, with $E_{p,a}$ varying 70−80 mV per unit increase in pH. Re-reduction of Os^{IV} is pH-independent.

Os(IV → VI) oxidation occurs at approximately +1.1 V at pH 0.5 (wave B) and is pH-dependent, with $E_{p,a}$ decreasing ~70 mV/pH unit as the pH is increased. The Os(VI → IV) reduction at wave II overlaps with the Os(III → II) wave at $E_{p,c} \approx -0.18$ V. Above pH 3.0, this wave is pH-dependent. It appears at $E_{p,c} = -0.45$ V at pH 7.

A similar pattern of waves was observed in CD_3CN to which an excess of 2,2′-bipyridine was added as a base (Figure 4). Os(III → IV) oxidation at wave A becomes irreversible and shifts to lower potential. On a reverse scan after cycling through this wave, an Os(IV → III) reduction wave appears at $E_{p,c} = +0.16$ V (wave I). An oxidative scan through the Os(IV → VI) wave at $E_{p,a} \approx 1.7$ V results in the appearance of the irreversible Os(VI → V) reduction wave for *trans*-$[Os(tpy)(Cl)_2(N)]^+$ at $E_{p,c} = -0.32$ V (wave II).[18]

(18) (a) Demadis, K. D.; Meyer, T. J.; White, P. S. *Inorg. Chem.* **1997**, *36*, 5678. (b) Demadis, K. D.; El-Samanody, E.-S.; Meyer, T. J.; White, P. S. *Inorg. Chem.* **1998**, *37*, 838. (c) Demadis, K. D.; Meyer, T. J.; White, P. S. *Inorg. Chem.* **1998**, *37*, 3610.

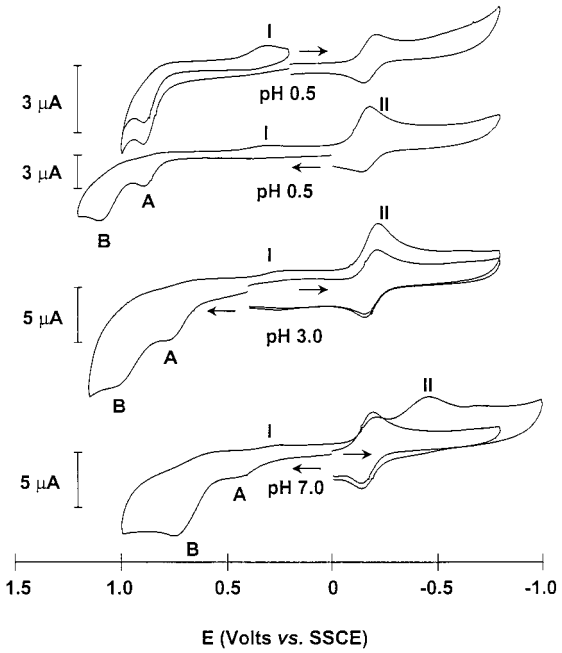

Figure 3. Cyclic voltammograms of *trans*-[Os(tpy)$(Cl)_2(NH_3)$](PF_6). Conditions as in Figure 2.

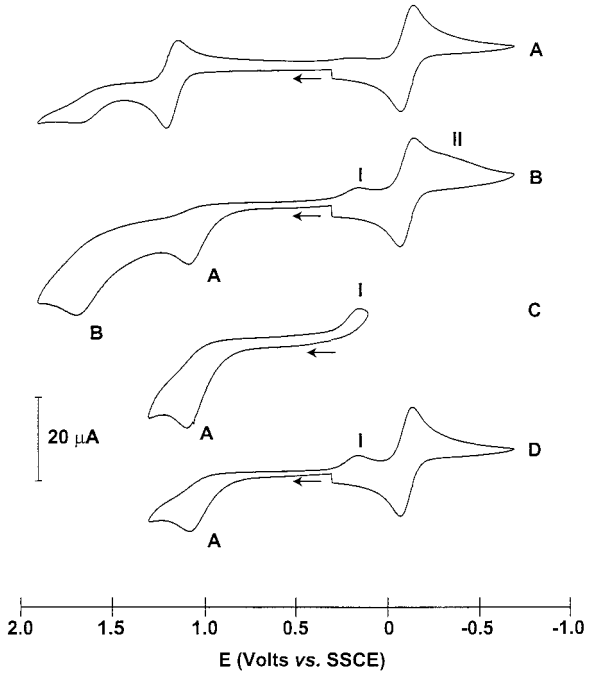

Figure 4. Cyclic voltammograms of *trans*-[Os(tpy)$(Cl)_2(NH_3)$](PF_6), ~1 mM in acetonitrile solution, 0.1 M in TBAH. Potentials are vs SSCE. Voltammograms B, C, and D were recorded after addition of 25 mM 2,2′-bipyridine. The scan rate is 100 mV/s.

[Os(tpy)(bpy)(NH_3)]$(PF_6)_2$. At pH <2, only an Os(III → II) wave is observed, at $E_{1/2} = +0.40$ V (Figure 5). By pH 3.0, an Os(III → IV) oxidation wave appears at $E_{p,a} \approx +0.8$ V (wave A). After cycling through this wave, a new wave appears for Os(IV → III) reduction at $E_{p,c} \approx 0.1$ V (wave I). $E_{p,a}$ for wave A decreases by 70−80 mV/pH unit from pH 3.0 to 7.0, at which point it overlaps with the Os(III → II) wave. Wave I is pH-independent.

Oxidation to Os^{IV} is accompanied by the appearance of a pair of waves at $E_{p,c} \approx -0.3$ and $E_{p,c} \approx -0.6$ V (waves II and III, respectively). They correspond to reduction of [Os(tpy)(bpy)(NO)]$^{3+}$.[10]

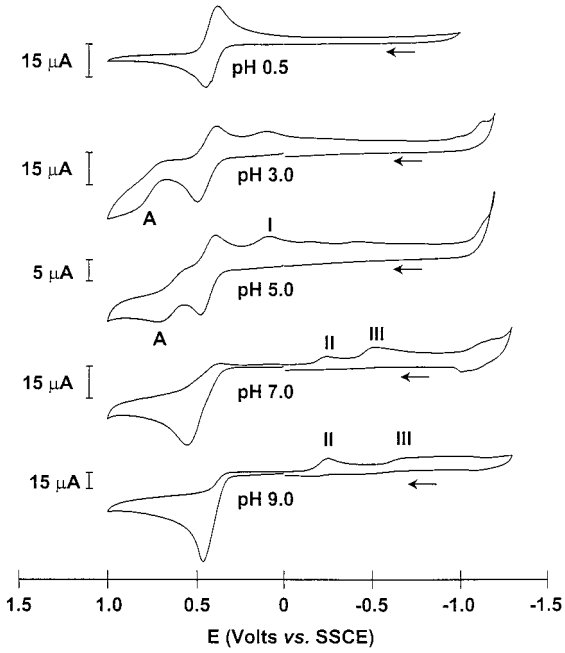

Figure 5. Cyclic voltammograms of [Os(tpy)(bpy)(NH_3)]$(PF_6)_2$, ~1 mM in aqueous solution. Potentials are vs SSCE. The scan rate is 100 mV/s.

$$[Os(tpy)(bpy)(NO)]^{3+} \xrightarrow{+e^-} [Os(tpy)(bpy)(NO^{\bullet})]^{2+} \quad (13)$$

$$[Os(tpy)(bpy)(NO^{\bullet})]^{2+} \xrightarrow{+e^-} [Os(tpy)(bpy)(NO^{-})]^{+} \quad (14)$$

When the scan rate is reduced or the electrode is held at a potential more positive than wave A at pH 5, waves II and III are enhanced at the expense of wave I. The nitrosyl complex is the ultimate product of oxidation at pH >2.[10]

***cis*-[Os(bpy)$_2$(Cl)(NH_3)](PF_6).** As shown in Figure 6, a chemically quasireversible Os(IV → III) wave is observed for this complex at $E_{1/2} = +1.23$ V at pH 0.5. From pH 1 to 5, this wave is obscured by background oxidation of water at the electrode. After an oxidative scan at pH 5.0, there is some evidence for Os(IV → III) reduction at $E_{p,c} \approx -0.2$ V (wave I). A reversible, pH-independent product wave appears at $E_{1/2} = +0.59$ V (wave B).

The Os(III → IV) wave reappears at pH 7 at $E_{p,a} \approx +0.5$ V (wave A). It is pH-dependent, with $E_{p,c}$ varying by ~120 mV/pH unit. By pH 9, it is irreversible and clearly multielectron in nature. A scan through this wave results in the appearance of wave B and new waves at $E_{p,c} \approx -0.45$ and $E_{p,c} \approx -0.70$ V (waves II and III, respectively). Exhaustive oxidation of *cis*-[Os(bpy)$_2$(Cl)(NH_3)]$^+$ at pH 9.0 gives *cis*-[Os(bpy)$_2$(Cl)(NO)]$^{2+}$ and the mixed-valence μ-N_2 dimer {*cis*-[Os(bpy)$_2$(Cl)]$_2$(μ-N_2)}$^{3+}$ in comparable amounts. The identity of the nitrosyl complex was confirmed by comparison of its IR and UV−visible spectra with those of an authentic sample ($\nu_{NO} = 1888$ cm^{-1} in KBr).[15,19] (See Table 2.) The origin of waves II and III is nitrosyl reduction. Wave B corresponds to the $Os^{III}Os^{II}$/$Os^{II}Os^{II}$ couple of the μ-N_2 complex (see below).

Dinitrogen Complexes. Electrochemical oxidation of solutions containing *cis*-[Os^{II}(bpy)$_2$(Cl)(NH_3)](PF_6) at pH 9 at potentials more positive than that of wave B in Figure 6 gives *cis*-[Os(bpy)$_2$(Cl)(NO)]$^{2+}$ and {*cis*-[Os(bpy)$_2$(Cl)]$_2$(μ-N_2)}$^{3+}$ ($Os^{III}Os^{II}$) as products. $Os^{III}Os^{II}$ is reduced to $Os^{II}Os^{II}$ ($n = 1$)

(19) For a general review of metal nitrosyls see: Richter-Addo, G. B.; Legzdins, P. *Metal Nitrosyls*; Oxford University Press: New York, 1992; see also references therein.

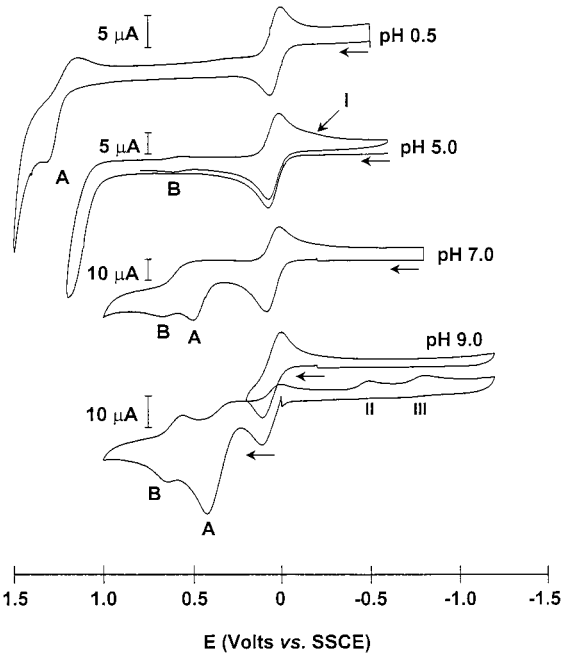

Figure 6. Cyclic voltammograms of *cis*-$[Os(bpy)_2(Cl)(NH_3)](PF_6)$. Conditions as in Figure 5.

when the applied potential is held more negative than that of wave B. $Os^{II}Os^{II}$ is stable indefinitely in solution and was isolated by precipitation of its PF_6^- salt. Cation exchange chromatography gave $Os^{II}Os^{II}$ as a 3:2 mixture of diastereomers, as determined by ^1H NMR.[20] Differences in the solubilities of the diastereoisomers may be responsible for their unequal abundance following workup (see Experimental Section).

Controlled-potential electrolysis at the same potential and pH as above, but with added NH_3/NH_4^+, gave mixtures of $Os^{III}Os^{II}$, *cis*-$[Os^{II}(bpy)_2(Cl)(NO)]^{2+}$, and *cis*-$[Os^{II}(bpy)_2(Cl)(N_2)]^+$. After reduction of $Os^{III}Os^{II}$ to $Os^{II}Os^{II}$, the components were separated from the mixture by cation exchange chromatography.

In cyclic voltammograms of $Os^{II}Os^{II}$ in CH_3CN, 0.1 M in TBAH, a wave appears at $E_{1/2} = 0.70$ V for the couple

$$[(bpy)_2(Cl)Os^{III}(N_2)Os^{II}(bpy)_2(Cl)]^{3+} \xrightarrow[-e^-]{+e^-} [(bpy)_2(Cl)Os^{II}(N_2)Os^{II}(bpy)_2(Cl)]^{2+} \quad (15)$$

The $Os^{III}Os^{II}$ form is stable for hours in acetonitrile. Chemical reversibility and *n* values were confirmed by coulometry. A second one-electron oxidation (by coulometry) occurs at $E_{p,a} = +1.4$ V, but the wave is irreversible up to scan rates of 5 V/s. The product is *cis*-$[Os^{III}(bpy)_2(Cl)(NCCH_3)]^{2+}$, $E_{1/2} = +0.41$ V ($Os^{III/II}$),[21] consistent with the reaction

$$[(bpy)_2(Cl)Os^{III}(N_2)Os^{II}(bpy)_2(Cl)]^{3+} \xrightarrow[+2CH_3CN]{-e^-,\ N_2} 2[Os^{III}(bpy)_2(Cl)(NCCH_3)]^{2+} \quad (16)$$

In acetonitrile, at scan rates of 100 mV/s, *cis*-$[Os(bpy)_2(Cl)(N_2)](PF_6)$ undergoes reversible, bipyridine-based reductions at $E_{1/2} = -1.30$ V and $E_{1/2} = -1.50$ V and an irreversible, metal-based oxidation at $E_{p,a} = +0.95$ V. Oxidation to Os^{III} is accompanied by loss of the dinitrogen ligand and coordination of acetonitrile, as shown by the appearance of the Os(III/II) wave for the CH_3CN complex.

$$cis\text{-}[Os^{II}(bpy)_2(Cl)(N_2)]^+ \xrightarrow[+CH_3CN]{-e^-,\ N_2} cis\text{-}[Os^{III}(bpy)_2(Cl)(NCCH_3)]^{2+} \quad (17)$$

UV−visible, infrared, and near-infrared spectra for the μ-N_2 complexes are reported elsewhere.[22]

In the resonance Raman spectrum of $Os^{II}Os^{II}$ in D_2O with 441.6-nm excitation, $\nu_{N\equiv N}$ appears as an intense band at 2053 cm^{-1} ($\Delta\bar{\nu}_{1/2} \approx 30$ cm^{-1}). It also appears in the IR at 2053 cm^{-1} in KBr.[23] For *cis,cis*-$[(bpy)_2(Cl)Os^{III}(N_2)Os^{II}(Cl)(bpy)_2](PF_6)_3$ in CH_3CN, 0.1 M in TBAH, $\nu_{N\equiv N}$ appears at 2008 cm^{-1} (2011 cm^{-1} in KBr). For *cis*-$[Os(bpy)_2(Cl)(N_2)](PF_6)$ in KBr, $\nu_{N\equiv N}$ appears as a sharp band at 2099 cm^{-1}.

Discussion

For a series of Os^{III} haloammine complexes, Buhr and Taube observed that chemically reversible $Os^{III} \rightarrow Os^{IV}$ oxidation occurs.[5]

$$mer\text{-}Os(NH_3)_3(X)_3 \underset{+e^-}{\overset{-e^-}{\rightleftharpoons}} mer\text{-}[Os(NH_3)_3(X)_3]^+ \quad (18)$$

cis- and *trans*-$[Os(NH_3)_4(X)_2]^+$ also undergo reversible oxidation to Os^{IV}, but only in solutions in which the pH is well below the pK_a of coordinated ammonia. In more basic solutions, oxidation is irreversible, as shown by cyclic voltammetry. Oxidation of $[Os(NH_3)_5(X)]^{2+}$ and $[Os(NH_3)_6]^{3+}$ was found to be irreversible even in strongly acidic solutions.

The origin of the instability of Os^{IV} was investigated by product analysis and decomposition kinetics. In general, Os^{IV} ammines containing two or fewer halide ligands were unstable with respect to disproportionation into Os^{III} and Os^{VI}.

$$3Os^{IV} \rightarrow 2Os^{III} + Os^{VI} \quad (19)$$

The fate of Os^{VI} depended on the number of halide ligands. *cis*- and *trans*-$[Os(NH_3)_4(Cl)_2]^{2+}$ gave *trans*-dioxo products

$$3trans\text{-}[Os(NH_3)_4(Cl)_2]^{2+} + 2H_2O \rightarrow 2trans\text{-}[Os(NH_3)_4(Cl)_2]^+ + trans\text{-}[Os(O)_2(NH_3)_4]^{2+} + 4H^+ + 2Cl^- \quad (20)$$

and the hexaammine and monohaloammines gave nitrido products, such as

$$[Os(NH_3)_6]^{3+} \xrightarrow{-H^+,\ e^-} [Os(NH_3)_5(NH_2)]^{3+} \quad (21)$$

$$3[Os(NH_3)_5(NH_2)]^{3+} + H_2O + H^+ \rightarrow 2[Os(NH_3)_6]^{3+} + [Os(N)(NH_3)_4(H_2O)]^{3+} + NH_4^+ \quad (22)$$

On the basis of kinetic and cyclic voltammetric data, deprotonation of Os^{IV} ammine was invoked as the first step in each case.

(20) Pseudo-octahedral *cis*-$M(bpy)_2(X)(Y)$ complexes exist as enantiomeric pairs. The combination of like enantiomers gives rise to an isomer that has no symmetry element, whereas the isomer formed by the combination of unlike enantiomers contains a mirror plane.

(21) Kober, E. M.; Marshall, J. L.; Dressick, W. J.; Sullivan, B. P.; Caspar, J. V.; Meyer, T. J. *Inorg. Chem.* **1985**, *24*, 2755.

(22) Demadis, K. D.; El-Samanody, E.-S.; Coia, G. M.; Meyer, T. J. *J. Am. Chem. Soc.* **1999**, *121*, 535.

(23) Only one of the two diastereomers has a mirror plane. Also, reductions in symmetry caused by crystal packing in the solid state may lend IR intensity to the band.

Table 2. UV−Visible Band Maxima and Molar Extinction Coefficients for the Os^{II} and Os^{III} Ammine Complexes

salt or complex	$\pi \rightarrow \pi^*$ transitions λ, nm (ϵ, 10^3 M^{-1} cm^{-1})	other bands λ, nm (ϵ, 10^3 M^{-1} cm^{-1})
$[Os^{III}(tpy)(bpy)(NH_3)](PF_6)_3$[a]	252 (32), 262 (33), 274 (34), 316 (27)	376[c] (4.6)
$[Os^{II}(tpy)(bpy)(NH_3)](PF_6)_2$[a]	234 (28), 278 (32), 292 (36), 320 (40)	404 (7.2), 500[c] (11), 580 (4.2), 754 (2.2)
cis-$[Os^{III}(bpy)_2(Cl)(NH_3)](PF_6)_2$[a]	252 (25), 286[c] (29)	352 (5.7), 384[c] (5.5)
cis-$[Os^{II}(bpy)_2(Cl)(NH_3)](PF_6)$[a]	246 (22), 296 (52)	368 (9.2), 442 (8.8), 528 (10), 768 (3.3)
trans-$[Os^{III}(tpy)(Cl)_2(NH_3)](PF_6)$[b]	278 (18), 322 (21)	404 (2.5), 464 (2.8), 518 (1.7), 556 (1.2), 672 (0.4)
trans-$[Os^{II}(tpy)(Cl)_2(NH_3)]$[b]	264 (17), 288 (17), 330 (20)	388 (7.1), 428 (6.6), 502 (6.4), 754 (2.4)
cis-$[Os^{III}(tpy)(Cl)_2(NH_3)](PF_6)$[b]	278 (21), 316 (23)	412 (3.0), 464[c] (3.8), 678 (0.5)
cis-$[Os^{II}(tpy)(Cl)_2(NH_3)]$[b]	264 (18), 286 (19), 330 (22)	402[c] (8.2), 414 (8.2), 506[c] (5.9), 622 (3.7), 690 (2.9)
cis-$[Os^{II}(bpy)_2(Cl)(N_2)](PF_6)$	236 (24), 290 (54)	350 (8.4), 410 (8.3), 500 (8.8), 690 (2.8)[d]

[a] Measured in acetonitrile. [b] Measured in dimethyl sulfoxide. [c] Most intense peak of a structured band. [d] Very broad.

$$[Os^{IV}(L)_5(NH_3)]^n \rightleftharpoons Os^{IV}(L)_5(NH_2)]^{n-1} + H^+ \quad (23)$$

Chemical or electrochemical oxidation of $[Os(NH_3)_5(CO)]^{2+}$ leads to a μ-N_2 complex.[24]

$$2[Os(NH_3)_5(CO)]^{2+} \xrightarrow{-6H^+,\,-6e^-} [(NH_3)_4(CO)Os]_2(N_2)]^{4+} \quad (24)$$

This reaction occurs by disproportionation of Os^{III}

$$2[Os(NH_3)_5(CO)]^{3+} \rightarrow [Os(NH_3)_5(CO)]^{2+} + [Os(NH_2)(NH_3)_4(CO)]^{3+} + H^+ \quad (25)$$

followed by further oxidation, proton loss, and coupling. The participation of higher oxidation states of osmium was inferred by the inhibition of μ-N_2 formation in the presence of thiourea added as a reductant.

The complexes used in this study differ from polyammines in that there is a single NH_3 ligand. They are substitutionally inert, which avoids complications arising from ligand substitution as in eqs 21 and 23, for example. Relative to NH_3, polypyridyl ligands withdraw more electron density from Os^{II} via $d\pi \rightarrow \pi^*$ back-bonding. In comparable coordination environments, this has the effect of stabilizing Os^{II}, which increases Os(III/II) potentials and which should enhance the acidity of bound NH_3.

Coordinated chloride ion stabilizes higher oxidation states by σ and π donation and by decreased charge, all of which contribute to decreasing $E_{1/2}$ values. This can be seen in the $E_{1/2}(Os^{III/II})$ values for the series from $[Os(tpy)(bpy)(NH_3)]^{2+}$ to $[Os(tpy)(Cl)_2(NH_3)]^+$, which decrease from +0.68 to −0.10 V in CH_3CN vs SSCE (Table 1). As a second example, $E_{1/2}$ for the $Os^{IV/III}$ couples of *cis*-$[Os(bpy)_2(Cl)(NH_3)]^+$ and *trans*-$[Os(tpy)(Cl)_2(NH_3)]^+$ are approximately +1.7 and +1.18 V.

These changes in coordination environment, and the concomitant changes in electron content at the metal, have a profound impact on reactivity and on the manner in which coordinated ammonia is oxidized.

Oxidation of Coordinated NH_3. Oxidation of coordinated NH_3 requires deprotonation. This is shown by the fact that *cis*- and *trans*-$[Os^{IV}(tpy)(Cl)_2(NH_3)]^{2+}$ are stable in CH_3CN or in acidic aqueous solution, at least on the cyclic voltammetry time scale. They undergo further oxidation only with the addition of 2,2′-bpy to CH_3CN or with an increase in the pH for the latter.

The key intermediates in this chemistry are deprotonated forms of Os(IV). They are reached either by deprotonation of Os^{III}-NH_3 followed by oxidation or by oxidation to Os^{IV}-NH_3 followed by deprotonation. These intermediates lead to the final products via four separate pathways: (1) In pathway 1, further oxidation and proton loss occurs to give stable Os^{VI}-nitrido products. The high oxidation state is stabilized by Os−nitrogen multiple bonding. For example, the Os−N bond distance in *trans*-$[Os^{VI}(tpy)(Cl)_2(N)]^+$ is 1.663(5) Å, consistent with an Os≡N triple bond.[7] (2) In pathway 2, N···N coupling and subsequent oxidation lead to μ-N_2 products. (3) In pathway 3, the nitrogen atom is sufficiently electron-deficient that hydration occurs. Hydration followed by further oxidation leads to nitrosyl products. (4) In pathway 4, an Os^{VI}-nitrido product is also obtained but by disproportionation of Os^{IV} into Os^{VI} and Os^{III} rather than by direct oxidation.

Scheme 1

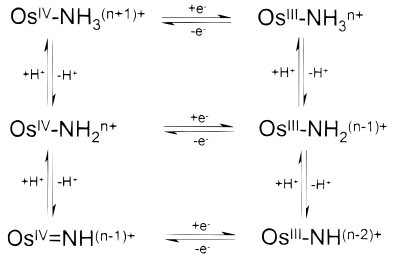

Oxidation Mechanism. Os^{III} to Os^{IV}. In the absence of proton-coupled electron transfer with the electrode, Os^{III} oxidation to Os^{IV} must occur by some combination of reactions in the "square scheme" in Scheme 1.[25] Protons must be lost in the net sense; the importance of proton loss for accessing the higher oxidation states has already been mentioned.

An important indication of proton involvement in the electrode reactions is the pH dependence of the voltammetric waves. For an electrochemically reversible process in which there is a change in proton content between oxidation states, $E_{1/2}$ for a pH-dependent couple is related to the formal potential for the related pH-independent couple ($E^{\circ\prime}$) by the Nernst equation.

$$E_{1/2} = E^{\circ\prime} - \frac{0.059m}{n}\,\mathrm{pH} \quad (26)$$

In this equation m and n are the numbers of protons and electrons transferred, respectively. Application to an irreversible process is only approximate.

The various possibilities for the origin of the pH dependences for the Os(III → IV) and Os(IV → III) couples in this work are listed in Chart 1. Chart 1 summarizes the pH dependences predicted for four different mechanistic cases. Each is labeled according to the rate-determining step and the pH dependences predicted for the Os(III → IV) and Os(IV → III) couples. In

(24) (a) Buhr, J. D.; Taube, H. *Inorg. Chem.* **1979**, *18*, 2208. (b) Buhr, J. D.; Taube, H. *Inorg. Chem.* **1980**, *19*, 2425.

(25) Bard, A. J.; Faulkner, L. R. *Electrochemical Methods: Fundamentals and Applications*; John Wiley & Sons: New York, 1980.

Chart 1

	reaction	pH dependence Os(III→IV)	pH dependence Os(IV→III)
(a)	$Os^{III}\text{-}NH_3^{n+} \underset{+e^-}{\overset{-e^-}{\rightleftharpoons}} Os^{IV}\text{-}NH_3^{(n+1)+}$ (RDS) $Os^{IV}\text{-}NH_3^{(n+1)+} + H_2O \rightleftharpoons Os^{IV}\text{-}NH_2^{(n-1)+} + H_3O^+$ (rapid)	no	yes
(b)	$Os^{III}\text{-}NH_3^{n+} + OH^- \rightleftharpoons Os^{III}\text{-}NH_2^{(n-1)+} + H_2O$ (RDS) $Os^{III}\text{-}NH_2^{(n-1)+} \underset{+e^-}{\overset{-e^-}{\rightleftharpoons}} Os^{IV}\text{-}NH_2^{n+}$ (rapid)	yes	no
(c)	$Os^{III}\text{-}NH_3^{n+} + 2OH^- \rightleftharpoons Os^{III}{=}NH^{(n-2)+} + 2H_2O$ (RDS) $Os^{III}{=}NH^{(n-2)+} \underset{+e^-}{\overset{-e^-}{\rightleftharpoons}} Os^{IV}{=}NH^{(n-1)+}$ (rapid)	yes	no
(d)	$Os^{III}\text{-}NH_3^{n+} + 2\,H_2O \underset{+e^-}{\overset{-e^-}{\rightleftharpoons}} Os^{IV}{=}NH^{(n-1)+} + 2H_3O^+$ [a]	yes	yes

[a] The rate-determining step is diffusion or diffusion kinetically coupled with electron−proton transfer.

(a), oxidation to Os^{IV} is rate-limiting, and the pH dependence arises from proton loss from Os^{IV} in a rapid acid−base equilibrium following oxidation. In (b) and (c), rate-limiting proton loss from Os^{III} to OH^- precedes oxidation. In (d), electron transfer is diffusionally limited or kinetically coupled to diffusion.

A significant difference in acidity is expected between the Os^{III} ammine and Os^{IV} ammine complexes. This is illustrated by the difference in the pK_a values for $[Pt(NH_3)_6]^{4+}$ (pK_a = 6.96) and $[Rh(NH_3)_6]^{3+}$ (pK_a > 14), for example.[27] When ligand pπ to metal dπ donation is possible, the effect is even more pronounced. The *organo*amine complexes $[Os(en)_3]^{4+}$ and $[Os(tmen)_3]^{4+}$ both exhibit pK_a's $\ll 0$.[26a−d] As a result, salts of these complexes are isolated in a deprotonated state, such as $[Os(en\text{-}H)_2(en)]^{4+}$. In cases in which structural information is available, bonds from the metal to the deprotonated nitrogen atom are short (1.90 Å in the last example). Strong evidence exists for the participation of related Ru^{IV} intermediates in the oxidative dehydrogenation of coordinated primary amines.[26e]

Another useful relationship is given in eq 27. It relates $E_{1/2}$ values to peak potentials for cases in which electron transfer is followed by a rapid chemical reaction. It allows $E_{1/2}$ values to be estimated for irreversible processes. In eq 27, $E_{p/2}$ is the half-peak potential, and n is the number of electrons transferred.[25]

$$E_{1/2} = E_{p/2} - \frac{28.0}{n}\,\text{mV} \qquad (27)$$

Oxidation of *cis*-$[Os^{III}(tpy)(Cl)_2(NH_3)]^+$. At pH 0.5, proton loss from the cis isomer occurs after or competitively with oxidation to Os^{IV}. On a reverse scan, reductive waves appear both for $Os^{IV}\text{−}NH_3^{2+}$ at $E_{p,c}$ = 0.80 V and for a deprotonated form at $E_{p,c}$ = 0.65 V. The pH dependence of the latter is consistent with case (a) in Chart 1 with $E_{p,c}$ for Os(IV → III) reduction decreasing 60−70 mV per unit increase in pH. With the caveat noted about applying eq 26 to irreversible processes, this is near the limiting value of 59 mV/pH unit predicted for transfer of one proton per electron. Assuming that one proton is lost following rate-limiting electron transfer, the mechanism becomes

$$cis\text{-}[Os^{III}(tpy)(Cl)_2(NH_3)]^+ \underset{+e^-}{\overset{-e^-}{\rightleftharpoons}} cis\text{-}[Os^{IV}(tpy)(Cl)_2(NH_3)]^{2+} \qquad (28)$$

$$cis\text{-}[Os^{IV}(tpy)(Cl)_2(NH_3)]^{2+} + H_2O \rightleftharpoons cis\text{-}[Os^{IV}(tpy)(Cl)_2(NH_2)]^+ + H_3O^+ \qquad (29)$$

The latter reaction can be written in a kinetically equivalent form.

$$cis\text{-}[Os^{IV}(tpy)(Cl)_2(NH_3)]^{2+} + OH^- \rightleftharpoons cis\text{-}[Os^{IV}(tpy)(Cl)_2(NH_2)]^+ + H_2O \qquad (29b)$$

For the microscopically reverse Os(IV → III) reduction, electron transfer is preceded by rapid proton loss, which accounts for the pH dependence. The base for the released proton could be either H_2O or OH^-.

Oxidation of *trans*-$[Os^{III}(tpy)(Cl)_2(NH_3)]^+$. Oxidation of the trans isomer to Os^{IV} is pH-dependent even at pH 0.5, with $E_{p,a}$ decreasing 70−80 mV/pH unit as the pH is increased. The reverse Os(IV → III) reduction at $E_{p,c}$ = +0.25 V is pH-independent from pH 0.5 to 7.0.

These observations are consistent with case (b) in Chart 1. The rate-limiting step in oxidation is proton loss from Os^{III} to OH^- before oxidation can occur.

$$trans\text{-}[Os^{III}(tpy)(Cl)_2(NH_3)]^+ + OH^- \rightleftharpoons trans\text{-}[Os^{III}(tpy)(Cl)_2(NH_2)]^0 + H_2O \qquad (30)$$

$$trans\text{-}[Os^{III}(tpy)(Cl)_2(NH_2)]^0 \underset{+e^-}{\overset{-e^-}{\rightleftharpoons}} trans\text{-}[Os^{IV}(tpy)(Cl)_2(NH_2)]^+ \qquad (31)$$

(26) (a) Lay, P. A.; Sargeson, A. M. *Inorg. Chim. Acta* **1992**, *200*, 449. (b) Lay, P. A.; Sargeson, A. M.; Skelton, B. W.; White, A. H. *J. Am. Chem. Soc.* **1982**, *104*, 6161. (c) Patel, A.; Ludi, A.; Bürgi, H.-B.; Raselli, A.; Bigler, P. *Inorg. Chem.* **1992**, *31*, 3405. (d) Bernhard, P.; Bull, D. J.; Bürgi, H.-B.; Osvath, P.; Raselli, A.; Sargeson, A. M. *Inorg. Chem.* **1997**, *36*, 2804. (e) Adcock, P. A.; Keene, F. R.; Smythe, R. S.; Snow, M. R. *Inorg. Chem.* **1984**, *23*, 2336.

(27) (a) Grunwald, E.; Fong, D.-W. *J. Am. Chem. Soc.* **1972**, *94*, 7371. (b) Klein, B.; Heck, L. *Z. Anorg. Allg. Chem.* **1975**, *416*, 269. (c) Novikov, L. K.; Kiprin, L. I.; Isaev, I. D.; Pashkov, G. L.; Mironov, V. E. *Zh. Prikl. Khim.* **1990**, *63*, 799. (d) Skibsted, L. H.; Ford, P. C. *Acta Chem. Scand.* **1980**, *A34*, 109. (e) Kretschmer, M.; Labouvie, L.; Quirin, K. W.; Wiehn, H.; Heck, L. *Z. Naturforsch.* **1980**, *35B*, 1096.

For Os(IV → III) reduction, electron transfer is rapid, and there is no pH dependence because H_2O acts as the acid to protonate $Os^{III}-NH_2^0$. Application of eq 27 gives $E_{1/2} \approx 0.2$ V for the *trans*-$[Os(tpy)(Cl)_2(NH_2)]^{+/0}$ couple. The change to rate-limiting proton loss to OH^- occurs because Os^{III} is less acidic than Os^{IV}. Proton loss requires OH^- rather than water as the base.

The difference in behavior between *cis*- and *trans*-$[Os^{III}(tpy)(Cl)_2(NH_3)]^+$ suggests that coordinated NH_3 is less acidic in the cis isomer than in the trans isomer. This may be due to an electronic trans effect. The NH_3 group is trans to tpy in the trans isomer and trans to Cl^- in the cis isomer (see Figure 1).

Oxidation of *cis*-$[Os^{II}(bpy)_2(Cl)(NH_3)]^+$. $E_{p,a}$ for Os(III → IV) oxidation decreases by ~120 mV/pH unit from pH 0.5 to 7, consistent with the loss of two protons from Os^{III} prior to electron transfer. There is evidence for Os(IV → III) reduction at $E_{p,c} = -0.2$ V at pH 5.0, but Os^{IV} does not build up as a significant intermediate. Assuming that OH^- is the base, this is case (c) in Chart 1. The mechanism involves rate-determining loss of *two* protons followed by oxidation.

$$cis\text{-}[Os^{III}(bpy)_2(Cl)(NH_3)]^{2+} + OH^- \rightleftharpoons cis\text{-}[Os^{III}(bpy)_2(Cl)(NH_2)]^+ + H_2O \quad (32)$$

$$cis\text{-}[Os^{III}(bpy)_2(Cl)(NH_2)]^+ + OH^- \rightleftharpoons cis\text{-}[Os^{III}(bpy)_2(Cl)(NH)]^0 + H_2O \quad (33)$$

$$cis\text{-}[Os^{III}(bpy)_2(Cl)(NH)]^0 \underset{+e^-}{\overset{-e^-}{\rightleftharpoons}} cis\text{-}[Os^{IV}(bpy)_2(Cl)(NH)]^+ \quad (34)$$

In the oxidation of a Ru ammine cage complex to an imine form, evidence for both singly and doubly deprotonated Ru^{IV} intermediates has been found.[26]

Oxidation of $[Os^{III}(tpy)(bpy)(NH_3)]^{3+}$. An Os(III → IV) wave that is pH-dependent is observed by pH 3, with $E_{p,a}$ varying ~70 mV/pH unit. Os(IV → III) reduction at $E_{p,c} \approx 0.1$ V is pH-independent. This is also an example of case (b) in Chart 1, with rate-limiting proton transfer to OH^- followed by electron transfer.

$$[Os^{III}(tpy)(bpy)(NH_3)]^{3+} + OH^- \rightleftharpoons [Os^{III}(tpy)(bpy)(NH_2)]^{2+} + H_2O \quad (35)$$

$$[Os^{III}(tpy)(bpy)(NH_2)]^{2+} \underset{+e^-}{\overset{-e^-}{\rightleftharpoons}} [Os^{IV}(tpy)(bpy)(NH_2)]^{2+} \quad (36)$$

Application of eq 27 gives $E_{1/2} \approx 0.1$ V for the $[Os(tpy)(bpy)(NH_2)]^{3+/2+}$ couple.

Overview. The electrochemical data reveal the importance of deprotonation in stabilizing Os^{IV}, at least in terms of providing access to this unstable oxidation state. For the $[Os(tpy)(bpy)(NH_3)]^{4+/3+}$ couple, $E_{1/2} > 1.2$ V, compared to $E_{1/2} \approx 0.1$ V for the $[Os(tpy)(bpy)(NH_2)]^{3+/2+}$ couple, $E_{1/2} = 0.88$ V for the *trans*-$[Os(tpy)(Cl)_2(NH_3)]^{2+/+}$ couple, and $E_{1/2} \approx 0.2$ V for the *trans*-$[Os^{IV}(tpy)(Cl)_2(NH_2)]^{+/0}$ couple. A similar stabilization occurs for aqua/hydroxo couples. For the *cis*-$[Ru(bpy)_2(py)(OH_2)]^{3+/2+}$ couple, $E_{1/2} = 1.06$ V, compared to $E_{1/2} = 0.30$ V for the *cis*-$[Ru(bpy)_2(py)(OH)]^{2+/+}$ couple.[1b] Deprotonation decreases the charge on the complex and stabilizes higher oxidation states via $p\pi \rightarrow d\pi$ electron donation from the deprotonated ligands.

Although the conclusions reached concerning proton content at Os^{IV} must be regarded as tentative, loss of two protons to give the nitrene, *cis*-$[Os^{IV}(bpy)_2(Cl)(NH)]^+$, would provide further stabilization by $p\pi \rightarrow d\pi$ multiple bonding. Multiple bonding plays an important role in stabilizing high-oxidation-state oxo complexes such as *cis*-$[Ru^{IV}(bpy)_2(py)(O)]^{2+}$.

Because of the kinetic barriers imposed by the gain or loss of protons from nitrogen, there are no examples of electrochemically reversible or even quasireversible couples such as *cis*-$[Os^{IV}(tpy)(Cl)_2(NH_2)]^+$/*cis*-$[Os^{III}(tpy)(Cl)_2(NH_3)]^+$ in which there is a change in proton content between oxidation states. This is case (d) in Chart 1. Analogous hydroxo/aqua couples such as *cis*-$[Ru^{III}(bpy)_2(py)(OH)]^{2+}$/*cis*-$[Ru^{II}(bpy)_2(py)(H_2O)]^{2+}$ are reversible because proton gain or loss from oxygen is kinetically more facile.[1b]

Reactions of Os^{IV}. Os^{IV} is an unstable oxidation state in all cases. It exhibits a remarkable diversity of reactions that depend intimately on the electron content at the metal.

As reflected in the $Os^{III/II}$ potentials in Table 1, *cis*- and *trans*-$[Os^{III}(tpy)(Cl)_2(NH_3)]^+$ are relatively electron-rich. They undergo further oxidation at higher potentials to give Os^{VI}.

$$[Os^{IV}(tpy)(Cl)_2(NH_2)]^+ \underset{+2e^-,\,+2H^+}{\overset{-2e^-,\,-2H^+}{\rightleftharpoons}} [Os^{VI}(tpy)(Cl)_2(N)]^+ \quad (37)$$

These reactions are analogous to the oxidation of oxo/aqua complexes to even higher oxidation states. These reactions also occur with proton loss and stabilization by formation of an additional oxo group.[28]

$$[Os^{IV}(tpy)(H_2O)_2(O)]^{2+} \underset{+2e^-,\,+2H^+}{\overset{-2e^-,\,-2H^+}{\rightleftharpoons}} trans\text{-}[Os^{VI}(tpy)(O)_2(H_2O)]^{2+} \quad (38)$$

In these reactions, coordinated NH_3 and H_2O play a fundamental role because of their dissociable protons. Loss of protons in the higher oxidation states frees electron pairs in $2p\pi$ orbitals on bound oxygen or nitrogen for donation to the electron-deficient metal. With coordinated NH_3, loss of four electrons and three protons is sufficient to stabilize Os^{VI} via $Os{\equiv}N$ triple bonding. With coordinated H_2O, two bound H_2O molecules are required with dioxo formation resulting in two double bonds.

In the absence of further oxidation, the Os^{IV} forms of *cis*- and *trans*-$[Os^{III}(tpy)(Cl)_2(NH_3)]^+$ are unstable with respect to disproportionation.

$$3[Os^{IV}(tpy)(Cl)_2(NH_2)]^+ \rightarrow 2[Os^{III}(tpy)(Cl)_2(NH_3)]^+ + [Os^{VI}(tpy)(Cl)_2(N)]^+ \quad (39)$$

These reactions occur on the time scale of seconds under the conditions of the cyclic voltammetry experiments, and this has prevented further characterization. The mechanism of disproportionation is currently under investigation.

For *cis*-$[Os^{IV}(bpy)_2(Cl)(NH)]^+$ and $[Os^{IV}(tpy)(bpy)(NH_2)]^+$, further oxidation to Os^{VI} is inaccessible within the solvent limit. Disproportionation does not occur because of the inaccessibility of Os^{VI}. These complexes are unstable toward hydration and further oxidation to give nitrosyl products. For $[Os^{IV}(tpy)(bpy)(NH_2)]^{3+}$, the nitrosyl complex forms on the cyclic voltammetry time scale of seconds even in acidic solution. The net reaction is

(28) (a) Pipes, D. W.; Meyer, T. J. *J. Am. Chem. Soc.* **1984**, *106*, 7653. (b) Pipes, D. W.; Meyer, T. J. *Inorg. Chem.* **1986**, *25*, 4042.

$$[Os^{IV}(tpy)(bpy)(NH_2)]^{3+} + H_2O \xrightarrow{-4H^+,\,-4e^-} [Os^{II}(tpy)(bpy)(NO)]^{3+} \quad (40)$$

The mechanism of this reaction is unknown, but an oxygen atom must be added at some stage, possibly by hydration of the nitrogen atom of Os^{IV} to give bound hydroxylamine.

$$[Os^{IV}(tpy)(bpy)(NH_2)]^{3+} + H_2O \rightarrow [Os^{II}(tpy)(bpy)(NH_2OH)]^{2+} + H^+ \quad (41)$$

This can be viewed as an internal redox reaction in which electron transfer, triggered by hydration, occurs from nitrogen to Os^{IV}. Stable Ru^{II} and Os^{II} complexes containing coordinated hydroxylamine have been reported.[29]

There is an analogous chemistry for amines. Oxidation of $[Os^{II}(tpy)(bpy)(NH_3)]^{2+}$ in aqueous solutions containing secondary amines produces hydrazine complexes as intermediates.[11]

$$[Os^{IV}(tpy)(bpy)(NH_2)]^{3+} + HNEt_2 \rightarrow [Os^{II}(tpy)(bpy)(NH_2NEt_2)]^{2+} + H^+ \quad (42)$$

These complexes undergo further oxidation to give isolable hydrazido products.[11]

$$[Os^{II}(tpy)(bpy)(NH_2NEt_2)]^{2+} \xrightarrow{-2H^+,\,-2e^-} [Os^{IV}(tpy)(bpy)(NNEt_2)]^{2+} \quad (43)$$

Further oxidation of the putative hydroxylamine intermediate would lead to the final nitrosyl product.

$$[Os^{II}(tpy)(bpy)(NH_2OH)]^{2+} \xrightarrow{-2H^+,\,-2e^-} [Os(tpy)(bpy)(NHO)]^{2+} \quad (44)$$

$$[Os(tpy)(bpy)(NHO)]^{2+} \xrightarrow{-H^+,\,-2e^-} [Os(tpy)(bpy)(NO)]^{3+} \quad (45)$$

Twice-deprotonated hydroxylamine (NHO^{2-}) has been identified as a ligand in an Os^{IV} complex.[30]

Hydration of the electron-deficient N atom appears to be base-catalyzed, as shown by the growth in waves II and III at the expense of wave I as the pH is increased. In base, OH^- may serve as the nucleophile

$$[Os^{IV}(tpy)(bpy)(NH_2)]^{3+} + OH^- \rightarrow [Os^{II}(tpy)(bpy)(NH_2OH)]^{2+} \quad (46)$$

or it may remove a second proton to give the nitrene

$$[Os^{IV}(tpy)(bpy)(NH_2)]^{3+} + OH^- \rightarrow [Os^{IV}(tpy)(bpy)(NH)]^{2+} + H_2O \quad (47)$$

followed by hydration.

$$[Os^{IV}(tpy)(bpy)(NH)]^{2+} + H_2O \rightleftharpoons [Os^{II}(tpy)(bpy)(NH_2OH)]^{2+} \quad (48)$$

cis-$[Os^{IV}(bpy)_2(Cl)(NH)]^+$ is also unstable in acidic solution, but toward N···N coupling to give *cis,cis*-$[(bpy)_2(Cl)Os(N_2)Os(Cl)(bpy)_2]^{2+}$. This reaction presumably occurs through the diimine

$$2cis\text{-}[Os(bpy)_2(Cl)(NH)]^+ \rightarrow cis,cis\text{-}[(bpy)_2(Cl)Os(NH{=}NH)Os(Cl)(bpy)_2]^{2+} \quad (49)$$

followed by oxidation and proton loss.

$$cis,cis\text{-}[(bpy)_2(Cl)Os(NH{=}NH)Os(Cl)(bpy)_2]^{2+} \xrightarrow{-2H^+,\,-2e^-} cis,cis\text{-}[(bpy)_2(Cl)Os(N{\equiv}N)Os(Cl)(bpy)_2]^{2+} \quad (50)$$

A similar coupling scheme has been proposed by Collman and co-workers for intramolecular N···N coupling in a cofacial Ru diporphyrin complex.[31] Sellman et al. have isolated and structurally characterized dinuclear compounds containing bridging HN=NH.[32,33]

N···N coupling could also occur by attack of *cis*-$[Os^{IV}(bpy)_2(Cl)(NH)]^+$ on coordinated NH_3 in *cis*-$[Os^{III}(bpy)_2(Cl)(NH_3)]^{2+}$ or *cis*-$[Os^{II}(bpy)_2(Cl)(NH_3)]^+$. This seems unlikely because oxidation of *cis*-$[Os(bpy)_2(Cl)(NH_3)]^+$ in a large excess of NH_4^+ gives some *cis*-$[Os^{II}(bpy)_2(Cl)(N_2)]^+$ but mainly the μ-N_2 dimer.

The contrast in behavior between $[Os^{IV}(tpy)(Cl)_2(NH_2)]^+$ and *cis*-$[Os^{IV}(bpy)_2(Cl)(NH)]^+$ is striking. The first undergoes disproportionation and the second N···N coupling. An important factor influencing this difference may be the difference in proton content, with N···N coupling favored for the doubly deprotonated form. It is conceivable that, under strongly basic conditions, oxidation of $[Os(tpy)(Cl)_2(NH_3)]^+$ may lead to μ-N_2 products as well. Both *cis*- and *trans*-$[(tpy)(Cl)_2Os(N_2)Os(Cl)_2(tpy)]$ are known.[22]

As the pH is raised to 9.0, the nitrosyl, *cis*-$[Os(bpy)_2(Cl)(NO)]^{2+}$, becomes a competitive product. By inference, OH^- attack on the nitrene begins to compete with N···N coupling at this pH.

$$cis\text{-}[Os^{IV}(bpy)_2(Cl)(NH)]^+ \xrightarrow{+OH^-} cis\text{-}[Os^{II}(bpy)_2(Cl)(NH_2O)] \quad (51)$$

Further oxidation would give the nitrosyl.

$$cis\text{-}[Os(bpy)_2(Cl)(NH_2O)] \xrightarrow{-2H^+,\,-4e^-} cis\text{-}[Os^{II}(bpy)_2(Cl)(NO)]^{2+} \quad (52)$$

Oxidation Mechanism. *cis*- and *trans*-$[Os^{IV}(tpy)(Cl)_2(NH)]$ to *cis*- and *trans*-$[Os^{VI}(tpy)(Cl)_2(N)]^+$. In the absence of proton-coupled electron transfer to the electrode, oxidation of Os^{IV} to Os^{VI} must also occur by some combination of sequential electron- and proton-loss steps, such as these shown in Scheme 2. Given the conclusion that the proton composition at Os^{IV} is $Os^{IV}-NH_2^+$ for these complexes, two protons and two electrons must be lost to reach $Os^{VI}{\equiv}N^+$.

(29) Cheng, T.-Y.; Ponce, A.; Rheingold, A. L.; Hillhouse, G. L. *Angew. Chem., Int. Ed. Engl.* **1994**, *33*, 657.
(30) Wilson, R. D.; Ibers, J. A. *Inorg. Chem.* **1979**, *18*, 336.
(31) Collman, J. P.; Hutchison, J. E.; Lopez, M. A.; Guilard, R.; Reed, R. A. *J. Am. Chem. Soc.* **1991**, *113*, 2794.
(32) (a) Wurminghausen, T.; Sellman, D. *J. Organomet. Chem.* **1980**, *199*, 77. (b) Sellman, D. In *Nitrogen Fixation: Fundamentals and Applications*; Tikhonovich, I. A., Provorov, N. A., Romanov, V. I., Newton, W. E., Eds.; Kluwer Academic Publishers: Dordrecht, The Netherlands, 1995; p 123.
(33) Complexes with terminally bound diazene have also been reported: (a) Smith, M. R., III; Cheng, T.-Y.; Hillhouse, G. K. *J. Am. Chem. Soc.* **1993**, *115*, 8638. (b) Cheng, T.-Y.; Peters, J. C.; Hillhouse, G. K. *J. Am. Chem. Soc.* **1994**, *116*, 204.

Scheme 2

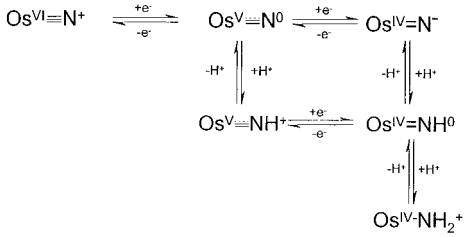

For the trans isomer, the decrease in $E_{p,a}$ for the Os(IV → VI) wave of ~70 mV per unit increase in pH is consistent with the loss of two protons and two electrons. Reduction of *trans*-$[Os^{VI}(tpy)(Cl)_2(N)]^+$ overlaps with the Os(III → II) wave for the $Os^{III/II}$ couple of *trans*-$[Os^{III}(tpy)(Cl)_2(NH_3)]^+$, but it appears to be pH-independent, at least from pH 0.5 to 3.0, and occurs at $E_{p,c} \approx -0.18$ V.

These observations are consistent with rate-limiting loss of the remaining protons from $Os^{IV}-NH_2^+$ to OH^- as the base, followed by electron transfer. Deprotonation before oxidation of Os^{IV} is also important in CH_3CN, as shown by the influence of added bpy in Figure 4.

$$trans\text{-}[Os^{IV}(tpy)(Cl)_2(NH_2)]^+ + OH^- \rightleftharpoons trans\text{-}[Os^{IV}(tpy)(Cl)_2(NH)]^0 + H_2O \quad (53)$$

$$trans\text{-}[Os^{IV}(tpy)(Cl)_2(NH)]^0 + OH^- \rightarrow trans\text{-}[Os^{IV}(tpy)(Cl)_2(N)]^- + H_2O \quad (54)$$

$$trans\text{-}[Os^{IV}(tpy)(Cl)_2(N)]^- \underset{+e^-}{\overset{-e^-}{\rightleftharpoons}} trans\text{-}[Os^{V}(tpy)(Cl)_2(N)]^0 \quad (55)$$

$$trans\text{-}[Os^{V}(tpy)(Cl)_2(N)]^0 \underset{+e^-}{\overset{-e^-}{\rightleftharpoons}} trans\text{-}[Os^{VI}(tpy)(Cl)_2(N)]^+ \quad (56)$$

There is no evidence for Os^V as an intermediate oxidation state, and further oxidation after deprotonation occurs by a net two-electron transfer to the electrode.

The behavior of Os^V in water contrasts to its behavior in acetonitrile, in which one-electron reduction of $[Os^{VI}(tpy)(Cl)_2(N)]^+$ to $[Os^{V}(tpy)(Cl)_2(N)]^0$ is followed by rapid N···N coupling to give $[(tpy)(Cl)_2Os(N_2)Os(Cl)_2(tpy)]$.[18,22] The difference may be that, in H_2O, further reduction to Os^{IV} is accompanied by protonation by H_2O (eq 54) to give $[Os(tpy)(Cl)_2(NH)]^+$. The instability of Os^V is probably attributable to its electronic configuration. In $[Os^{VI}(tpy)(Cl)_2(N)]^+$, the electronic configuration is $d\pi_1^2$. Reduction to Os^V occurs by addition of an electron to a $d\pi^*$ level, which is strongly antibonding with regard to the Os≡N interaction.[34]

Above pH 3, both $Os^{IV}-NH_2^+$ oxidation and $Os^{VI}\equiv N^+$ reduction are pH-dependent, with both waves varying ~70 mV/pH unit. Under these conditions, electron transfer and proton loss are kinetically coupled with diffusion, but both are slow, given the large peak-to-peak separation, with $\Delta E_p = E_{p,a}$(wave B) $- E_{p,c}$(wave II) = 0.6 V at pH 3.0 (Figure 3). Under these conditions the couple at the electrode is

$$trans\text{-}[Os^{VI}(tpy)(Cl)_2(N)]^+ + 2e^- + 2H^+ \rightarrow trans\text{-}[Os^{IV}(tpy)(Cl)_2(NH_2)]^+ \quad (57)$$

At the potential required for Os^{VI} reduction, reduction to Os^{IV} is followed by further reduction to Os^{III} and Os^{II}. For the couple in eq 57, $E_{1/2} \approx {}^1/_2[E_{p,a}$(wave B) $- E_{p,c}$(wave II)], which gives $E_{1/2} \approx +0.4$ V for the $Os^V\equiv N^+/Os^{IV}-NH_2^+$ couple at pH 3.0 and $E_{1/2} \approx +0.2$ V at pH 7.0.

Scheme 3

cis-$[Os^{III}(tpy)(Cl)_2(NH_3)]^+$ (at pH 7.0, μ = 0.1 M, 25 °C, *vs.* NHE; add 0.24 V *vs.* SSCE)

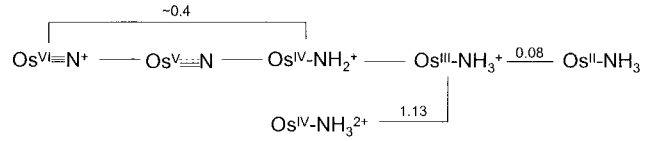

trans-$[Os^{III}(tpy)(Cl)_2(NH_3)]^+$

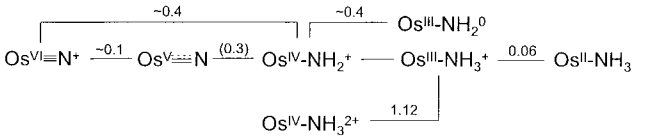

Os^V is an intermediate oxidation state and kinetic intermediate, but there is no direct evidence for it in the cyclic voltammograms. It is still possible to estimate $E_{1/2}$ for the Os(VI/V) couple on the basis of eq 27 and $E_{p,c} = -0.18$ V for wave II in Figure 3. This estimation gives $E_{1/2} \approx -0.1$ V for the *trans*-$[Os(tpy)(Cl)_2(N)]^{+/0}$ couple.

The same analysis can be applied to the oxidation of *cis*-$[Os^{IV}(tpy)(Cl)_2(NH_2)]^+$. Both $Os^{IV}-NH_2^+$ oxidation and $Os^{VI}\equiv N^+$ reduction are pH-dependent, with $E_{p,c}$ for the latter decreasing by 50−60 mV per unit increase in pH. This is consistent with the couple

$$cis\text{-}[Os^{VI}(tpy)(Cl)_2(N)]^+ + 2e^- + 2H^+ \rightarrow cis\text{-}[Os^{IV}(tpy)(Cl)_2(NH_2)]^+ \quad (58)$$

As calculated from ${}^1/_2[E_{p,c}$(wave B) $- E_{p,a}$(wave I)] in Figure 2, $E_{1/2} \approx +0.6$ V at pH 0.5 or $E_{1/2} \approx 0.2$ V at pH 7.0.

Latimer Diagrams.[35] Redox potentials for *cis*- and *trans*-$[Os^{III}(tpy)(Cl)_2(NH_3)]^+$ are summarized in the Latimer diagrams in Scheme 3. Potentials are cited at pH 7 vs NHE, which is −0.24 V relative to SSCE. The values obtained from measurements of irreversible couples must be regarded as tentative because of the assumptions made in deriving the $E_{1/2}$ values. Even the proton contents at Os^{IV} must be regarded as tentative. Values in parentheses were calculated from potentials for adjacent couples. The values for *trans*-$[Os^{III}(tpy)(Cl)_2(NH_3)]^+$ are different from those reported previously.[7] There were difficulties in the earlier study, one arising from trans → cis isomerization of the nitrido complex in water, which was not recognized until later. We have also changed the interpretation of some of the results on the basis of the current, more detailed pH-dependent results.

With these limitations recognized, some tentative but valuable conclusions can be reached about the redox properties of the various oxidation states. For both complexes, $[Os^{VI}(tpy)(Cl)_2(N)]^+$ is a relatively weak, two-electron oxidant at pH 7, but its potentials increase to ~0.8 V in 1 M acid. For the cis complex, Os^V is highly unstable with respect to disproportionation, with

(34) Ware, D. C.; Taube, H. *Inorg. Chem.* **1991**, *30*, 4605.

(35) Latimer, W. M. *Oxidation Potentials*, 2nd ed.; Prentice Hall: Englewood Cliffs, NJ, 1952.

$\Delta G^\circ \approx -0.8$ eV at pH 7.0 for the reaction

$$2cis\text{-}[Os^{V}(tpy)(Cl)_2(N)] + 2H^+ \rightarrow cis\text{-}[Os^{VI}(tpy)(Cl)_2(N)]^+ + cis\text{-}[Os^{IV}(tpy)(Cl)_2(NH_2)]^+ \quad (59)$$

Given the favorable driving force for this reaction, it is not surprising that Os^V does not appear as a significant intermediate.

Acknowledgment. The authors acknowledge the National Science Foundation for funding this research under Grant CHE-9503738 and Dr. Martin Devenney for obtaining the Raman spectrum of *cis,cis*-$[(bpy)_2(Cl)Os^{II}(N{\equiv}N)Os^{II}(Cl)(bpy)_2]^{2+}$.

Supporting Information Available: Figures with UV−visible spectroelectrochemical titration of *cis,cis*-$[(bpy)_2(Cl)Os^{II}(N_2)Os^{II}(bpy)_2(Cl)]^{2+}$ to *cis,cis*-$[(bpy)_2(Cl)Os^{III}(N_2)Os^{II}(bpy)_2(Cl)]^{3+}$ (Figure S-1) and resonance-Raman and infrared spectra of *cis,cis*-$[(bpy)_2(Cl)Os^{II}(N_2)Os^{II}(bpy)_2(Cl)]^{2+}$ and *cis,cis*-$[(bpy)_2(Cl)Os^{III}(N_2)Os^{II}(bpy)_2(Cl)]^{3+}$ (Figure S-2). This material is available free of charge via the Internet at http://pubs.acs.org.

IC0000505